Where is basalt in river sediments, and why does it matter?

Marion Garçon, Catherine Chauvel

Where is basalt in river sediments, and why does it matter?

Marion Garçon[1,2*], **Catherine Chauvel**[1,2]

[1] *Université Grenoble Alpes, ISTerre, F-38041 Grenoble, France*
[2] *CNRS, ISTerre, F-38041 Grenoble, France*

* Corresponding author.

Abstract

Weathering, erosion and mineralogical sorting processes modify the chemical and isotopic compositions of sediments relative to those of their source rocks. The way and extent to which those processes affect the geochemistry of sediments is however not yet fully understood. Here, we report trace element data as well as Nd, Hf and Pb isotopic compositions of sediments sampled at different water depths in the Ganges, Yamuna and Chambal Rivers draining the Deccan Traps basalts and the crystalline and sedimentary rocks from the Himalayan mountain range and the northern Indian shield.

Isotopic differences between surface and bed sediments sampled at the same location reach 6 ε_{Nd} and about 15 ε_{Hf} units, suggesting that suspended loads and bedloads do not carry similar provenance information. Such differences are explained by the combined effects of differential erosion and mineralogical sorting processes during fluvial transport. Materials eroded from basalts are preferentially transported in suspension near the river surface while materials eroded from more crystalline precursors are transported near the bottom of the river. This depth-dependent provenance within the river channel leads to an overrepresentation of basaltic materials in fine-grained suspended loads that are finally delivered into the ocean and become part of the oceanic terrigenous clays. By contrast, the proportion of basaltic materials in coarser sediments such as bedloads or turbidites is underestimated.

Our results have important consequences on the use of Nd, Hf and Pb isotopic compositions of sediments as provenance proxies because they indicate that all grain-size fractions must be taken into account to properly trace source compositions. They also suggest that upper continental crust estimates derived from fine-grained sediments, such as suspended loads, may be biased towards basaltic compositions if basaltic outcrops are present in the drainage area.

Keywords :

Neodymium; Hafnium; Lead; Isotopes; River sediments; Himalaya; Deccan Traps

1. Introduction

River sediments are essentially mixtures of particles and minerals derived from the erosion of rocks exposed in the catchment area. Their chemical and isotopic compositions are often used to trace sources, estimate the average composition of the drained area or determine chemical and physical erosion rates in large basins (e.g. Goldstein et al., 1984; Goldstein and Jacobsen, 1988; Asmerom and Jacobsen, 1993; Allègre et al., 1996; Galy et al., 2001; Clift et al., 2002; Singh and France-Lanord, 2002; Vance et al., 2003; Millot et al., 2004; Kamber et al., 2005; Richards et al., 2005; Roddaz et al., 2005; Belousova et al., 2006; Singh et al., 2008; Singh, 2009; Dhuime et al., 2011; Padoan et al., 2011; Lupker et al., 2011; 2012a). However, using sediments as such proxies requires a proper understanding of biases introduced by erosion and sedimentary processes on chemical and isotopic compositions. Some studies have previously shown that the geographical extend of the source rocks in the catchment area do not always match with the proportions deduced from the isotopic compositions of sediments (Allègre and Rousseau, 1984; Goldstein and Jacobsen, 1988; Kramers and Tolstikhin, 1997; Tricca et al., 1999; Steinmann and Stille, 2008; Dhuime et al., 2011). This is because some lithologies are more erodible than others and/or are affected differently by climates that favor either chemical or physical alteration of rocks. Besides, it has been shown that the hydrodynamic sorting of particles within the water column during fluvial transport introduces large fractionation of the chemical and isotopic messages carried by bedload and suspended load sediments (Lupker et al., 2011; Bouchez et al., 2011; Garzanti et al., 2010; 2011; Garçon et al., 2013a; 2013b; 2014). Here, we go one step further and evaluate the combined effects of (a) contrasting climate and rock erodibility in the catchment area of a large river system and (b)

71 isotopic fractionation caused by hydrodynamic sorting in the water column during fluvial transport.
72 We discuss trace element concentrations and Nd, Hf, Pb isotopic compositions of sediments
73 sampled at different water depths in the Ganges fluvial system that drains the Deccan Traps basalts
74 and the crystalline and sedimentary rocks of both the Himalayan range and the northern Indian
75 shield. We show that bedloads and suspended loads carry different provenance information and
76 discuss potential implications for worldwide terrigenous sediments.

77 **2. Geological setting and Sampling**

78 Sedimentary material was recovered at three different sampling sites along the Ganges fluvial
79 system (Figure 1). Samples include bedload and suspended load sampled at different water depths
80 in the Yamuna and Ganges Rivers as well as bank sediments and surface suspended loads from the
81 Chambal River. All samples were recovered at high flow during the monsoon season (July to
82 September) from 1996 to 2009. Bank sediments were sampled on the river shore while bedloads
83 were dredged up from the bottom of the rivers. Suspended loads were sampled at the same location
84 than bedloads, at the water surface or at different depths within the river channel. They were
85 recovered after filtration of about 5L of river water under pressure through 0.2 μm filters. Detailed
86 sampling techniques can be found in Galy et al. (2008) and Lupker et al. (2011).
87 The first sampling site is located in Bangladesh at the outflow of the Ganges River (Figure 1);
88 given its location, it integrates all sediments transported by the Ganges and its tributaries. The
89 drainage basin covers about one million km^2 and includes Quaternary fluvial deposits from the
90 Indo-Gangetic floodplain, variably metamorphosed crystalline and sedimentary rocks from both
91 the Himalayan mountain range and the northern Indian shield, and few basaltic rocks from the
92 Deccan Traps (Le Fort, 1975; Krishnan, 1982). At this location, the Deccan Traps basalts represent
93 only 4% of the total drained area. Major and trace element concentrations, as well as Nd, Hf and

94 Pb isotopic compositions of sediments sampled at this location have been previously published by
95 Lupker et al. (2012) and Garçon et al. (2013a; 2013b) but are reported for convenience in Table 1.
96 The two other sampling sites are both located upstream in the floodplain, in the Yamuna and in the
97 Chambal Rivers. At the Yamuna sampling site, the drainage basin consists of ~20% of basalts from
98 the Deccan Traps, ~40% of crystalline and sedimentary rocks from both the Himalayan mountain
99 range and the northern Indian shield and ~40% of Quaternary floodplain deposits, mostly derived
100 from the erosion of the Himalayas (Figure 1). At the Chambal sampling site, the Deccan Traps
101 basalts constitute 30% of the basin area, the crystalline and sedimentary rocks from the Indian
102 shield represent ~60% and the remaining 10% consists of Quaternary floodplain deposits
103 containing the erosion products of both the Deccan Traps basalts and the Indian shield (Figure 1).
104

105 **3. Analytical techniques**

106 All samples were powdered in agate bowls using a planetary ball mill. They were pre-treated for 2
107 days in HNO_3 14N on a hot plate at 130°C, then evaporated and digested in a HF-$HClO_4$ mixture in
108 PARR® bombs for 6 weeks at 140°C or one week at 200°C. After complete dissolution, trace
109 element concentrations and Nd-Hf-Pb isotopes were measured following the procedures described
110 by Chauvel et al. (2011). Repeated measurements of BR or BR-24 rock standards were used to
111 calibrate trace element concentrations. The validity and reproducibility of the trace element data is
112 estimated to be better than 5% for most elements based on the analyses of several complete
113 duplicates and repeated measurements of international rock standards as unknown samples,
114 including sedimentary materials such as JSd-2 (see Supplementary Table 1 for more details).
115 Neodymium, Hf, and Pb were isolated using ion chromatography (Chauvel et al., 2011). Total
116 procedural blanks were less than 100 pg for Nd, Hf and Pb. Isotopic compositions were measured

on a Nu Plasma HR MC-ICP-MS at the ENS Lyon (France). For Nd and Hf, mass bias corrections were performed using $^{146}Nd/^{144}Nd=0.7219$ and $^{179}Hf/^{177}Hf=0.7325$, respectively. The reproducibility (2σ) of the Ames-Rennes Nd and Ames-Grenoble Hf reference standards run every two or three samples was better than 40 ppm for $^{143}Nd/^{144}Nd$ and $^{176}Hf/^{177}Hf$ ratios. The analytical drift was corrected using the recommended values of 0.511961 for the Ames-Rennes Nd (Chauvel and Blichert-Toft, 2001) and 0.282160 for the Ames-Grenoble Hf (Chauvel et al., 2011). For Pb, mass fractionation bias was corrected using a thallium spike (White et al., 2000). The reproducibility of the NBS 981 reference standard run every two or three samples was better than 170 ppm for $^{208}Pb/^{204}Pb$, 130 ppm for $^{207}Pb/^{204}Pb$ and 90 ppm for $^{206}Pb/^{204}Pb$ ratios. Analytical drifts were corrected by standard-bracketing using the published values of Galer and Abouchami (1998) for the NBS 981 reference standard.

4. Results

Trace element concentrations and Nd, Hf, and Pb isotopic compositions of sediments from the Yamuna and Chambal Rivers are reported in Table 1 together with the previously published data for the Ganges sediments (Garçon et al., 2013a; 2013b).

Figure 2 shows spidergrams normalized to the average upper continental crust composition of Rudnick and Gao (2003) for the Yamuna and Chambal sediments. At a first order, the trace element contents of the sediments resemble those of the upper continental crust. Enrichment factors span a relatively small range of values from 0.3 to 3.8 for all trace elements (Figure 2). No significant trace element variation is noticed between the Chambal and Yamuna sediments but systematic discrepancies are observed between suspended loads and bedloads/bank sediments. Compared to bedloads and bank sediments, suspended loads show generally lower Zr, Hf but higher Cs, Rb, Ba, Pb, Li and transition element (Sc, V, Cr, Co, Ni, Cu, Zn) contents. These chemical differences, similar to those observed in the Ganges bedloads and suspended loads (Garçon et al., 2013a), are

well explained by mineral sorting processes that occur during the fluvial transport of sediments. High Zr-Hf concentrations in bedloads and bank sediments result from preferential concentration of zircons at the bottom of the river while high mobile and transition element concentrations in suspended loads are due to higher proportions of phyllosilicates and oxides in suspension within the water column (see Lupker et al., 2011; Garzanti et al., 2010; 2011 and Garçon et al., 2013a for further details). Bank sediment BR 938 from the Chambal River (gray dashed line in Figure 2) does not exhibit the typical trace element features of bedloads/bank sediments. Instead, its trace element pattern strongly resembles that of suspended loads with typical low Zr-Hf contents and high mobile and transition element concentrations. Major element concentrations published by Lupker et al. (2012b) showed that this particular sample is also characterized by a high Al_2O_3/SiO_2 ratio (i.e. 0.20) compared to values usually found in bedloads and bank sediments (i.e. $Al_2O_3/SiO_2 < 0.16$ according to Garçon et al., 2013a). This strongly suggests that BR 938 contains anomalously high proportions of Al_2O_3-rich clays and that its composition more likely reflects that of a suspended load. Finally, Figure 2 shows that, compared to the Ganges sediments, suspended loads from the Chambal and Yamuna Rivers generally have lower Zr, Hf, Nb, Ta and Light Rare Earth Element (LREE) contents together with higher transition element contents.

Nd and Hf isotopic compositions of the Yamuna and Chambal sediments span large ranges of values ($-16.6 < \varepsilon_{Nd} < -9.9$; $-24.2 < \varepsilon_{Hf} < -4.5$; Table 1) and are generally more radiogenic than the Ganges sediments ($-17.8 < \varepsilon_{Nd} < -16.8$; $-30.2 < \varepsilon_{Hf} < -18.8$; Table 1). At both sampling sites, suspended loads have more radiogenic Nd and Hf isotopic compositions than bedloads and bank sediments, excluding the outlier sample BR 938.

Lead isotopic compositions of the Yamuna and Chambal sediments range between 39.00 and 40.50 for $^{208}Pb/^{204}Pb$, 15.72 and 15.88 for $^{207}Pb/^{204}Pb$ and 18.71 and 19.96 for $^{206}Pb/^{204}Pb$. Suspended loads tend

to be less radiogenic than bedloads and bank sediments and all sediments from the Chambal and Yamuna rivers are generally less radiogenic than those from the Ganges ($39.99 < {}^{208}Pb/{}^{204}Pb < 42.45$; $15.87 < {}^{207}Pb/{}^{204}Pb < 16.11$; $19.78 < {}^{206}Pb/{}^{204}Pb < 22.16$).

5. Discussion

5.1. Chemical and isotopic variations as a function of water depth

5.1.1. Ganges sediments from the delta

Neodymium, Hf and Pb isotopic compositions of sediments sampled at different water depths in the Ganges River in Bangladesh are shown in yellow in Figure 3. The first remarkable feature is that the Nd isotopic compositions of the Ganges sediments do not change with water depth and exhibit a constant value at $\varepsilon_{Nd} \approx -17$. This value is indistinguishable from the average isotopic signature of river sediments sampled at the Himalayan front i.e. sediments draining exclusively the Himalayan mountain range (Garçon et al., 2013a), showing the overwhelming contribution of the crystalline and sedimentary Himalayan sources to the total sedimentary budget of the Ganges in the delta (Galy and France-Lanord, 2001). Using major element ratios, Lupker et al. (2012b) estimated that the contribution of the Deccan Traps basalts at the outflow of the Ganges in Bangladesh can be highly variable from year to year but is less than 4% in the Ganges sediments sampled in 2004, 2007 and 2008 and used in this study. A quick isotopic mass balance calculation between 4% sediment with an $\varepsilon_{Nd} \approx +5$ typical of Deccan Traps basalts and 96% sediment with the low ε_{Nd} typical of the Himalayan units ($\varepsilon_{Nd} \approx -17$) shows that the resulting value is indistinguishable from that of the Himalayan sources. Note that the contribution of erosion products from the northern Indian shield cannot be distinguished from that of the Himalayan units because they are isotopically equivalent (Parrish and Hodges, 1996). Similarly, the contributions of the Quaternary floodplain deposits having already reworked the erosion products of the Himalayas cannot be

188 distinguished from the actual contribution of the crystalline and sedimentary rocks from the
189 Himalayan mountain range because they share the same composition.
190 In contrast to Nd, ε_{Hf} and Pb isotopic ratios change with water depth in the Ganges profile (Figure
191 3): bottom sediments have lower ε_{Hf} and more radiogenic Pb isotopic ratios than the overlying
192 suspended loads. These differences result of a "heavy mineral effect" caused by hydrodynamic
193 sorting processes during sediment transport, with a preferential concentration of coarse and dense
194 minerals at the bottom of the river. Indeed, Garçon et al. (2013a; 2013b; 2014) showed that the
195 excess of zircon, monazite and allanite in both bedloads and bank sediments shifts the Hf and Pb
196 isotopic compositions of these sediments towards low ε_{Hf} and high Pb isotope ratios compared to
197 suspended loads.
198
199 **5.1.1. Chambal and Yamuna rivers draining the Deccan Traps**
200 Upstream in the floodplain, sediments from the Yamuna and Chambal Rivers are isotopically very
201 different from the Ganges River samples (Table 1, Figure 3). They have generally higher ε_{Nd} and ε_{Hf}
202 values and less radiogenic Pb isotopic ratios that can simply be explained by a higher contribution
203 of basaltic erosion products from the Indian Deccan Traps (Figure 3). The isotopic variations as a
204 function of water depth are however more surprising. First, excluding the outlier bank sediment
205 BR 938 that contains suspended load-type material (see section 4), the ε_{Nd} of the Yamuna and
206 Chambal sediments dramatically decrease with depth, from -10 at the surface to about -16 at the
207 bottom of the river, a feature unknown in the Ganges sediments. Second, the downward decrease
208 of ε_{Hf} and increase of Pb isotopic ratios are much larger than those observed for the Ganges
209 sediments. Differences between surface and bottom sediments in the Yamuna River reach almost
210 15 ε_{Hf} units (Figure 3) and cannot result from hydrodynamic processes alone, as it is the case in the

211 Ganges sediments (Garçon et al., 2013a). Indeed, explaining the very radiogenic ε_{Hf} of the Yamuna
212 and Chambal surface suspended loads by hydrodynamic sorting only would require these
213 sediments to be almost exclusively made of radiogenic Himalayan minerals such as epidote (ε_{Hf} =
214 +0.6, Garçon et al., 2014), garnet (ε_{Hf} = -3.1, Garçon et al., 2014) and magnetite (ε_{Hf} = -6.5, Garçon
215 et al., 2014), a requirement that is not supported by petrological observations under the binocular
216 microscope. Instead, such isotopic variations with depth suggest, together with the Nd isotopic
217 change, that surface suspended loads from both the Yamuna and Chambal Rivers include much
218 higher proportions of basaltic erosion products from the Deccan Traps than the bed sediments,
219 which are dominated by erosion products from the crystalline and sedimentary rocks of the
220 Himalayan range and the Indian shield (Figure 3).
221 This interpretation is further supported by the trace element concentrations of the sediments (Figure
222 2). Suspended loads from the Chambal and Yamuna Rivers are significantly enriched in transition
223 elements (i.e. Sc, V, Cr, Co, Ni, Cu, Zn) and depleted in incompatible elements (i.e. Zr, Hf, Nb, Ta
224 and LREE) compared to both the Ganges sediments and the bedloads/bank sediments from the
225 same rivers (Figure 2). These features are typical of the trace element signature of basalts and are
226 therefore consistent with the presence of higher amount of Deccan Traps material in the suspended
227 loads of the Yamuna and Chambal Rivers. Furthermore, Figure 4 illustrates the variations of two
228 trace element ratios (La/Sm and Ni/Hf) as a function of depth in the Yamuna, Chambal and Ganges
229 Rivers. La/Sm and Ni/Hf ratios of sediments can be used to distinguish crustal from basaltic sources
230 because magmatic processes significantly fractionate these two ratios: the Himalayan and Indian
231 crystalline and sedimentary rocks are typically characterized by high La/Sm and low Ni/Hf while
232 the Deccan Traps basalts exhibit low La/Sm and high Ni/Hf (see the green and red fields in Figure
233 4). The downward variations seen in Figure 4 of both La/Sm and Ni/Hf ratios in the Chambal and

234 Yamuna depth profiles are consistent with a decreasing proportion of basaltic erosion products
235 from the water surface to the bottom of the rivers.
236 Both isotopes and trace element data thus support the idea that bedloads and suspended loads from
237 the Yamuna and Chambal Rivers do not share similar provenance information. This can be
238 explained by the contrasting erosion style of the Deccan Traps basalts, subjected to higher chemical
239 erosion in the plain, versus the crystalline and sedimentary rocks from the Himalayas subjected to
240 higher physical erosion at high altitude. Indeed, previous studies suggest that the Deccan Traps
241 basalts are chemically more altered than the surrounding crystalline and sedimentary rocks (Dessert
242 et al., 2001; Das et al., 2005; Rengarajan et al., 2009). This leads to the formation of basaltic erosion
243 products enriched in montmorillonite, a fine and flaky clay mineral that tends to remain in
244 suspension in the water column (Jha et al., 1993). Derry and France-Lanord (1996), Singh et al.
245 (2008) and Lupker et al. (2012b) thus suggest that basaltic erosion products from the Deccan Traps
246 might be found in higher proportion in fine-grained sediments in the Ganges and the Bengal fan.
247 Our data further support these suggestions, showing that the erosion products of the more
248 weatherable basalts are likely finer and preferentially transported in suspension near the river
249 surface whereas the erosion products of the more resistant crystalline and sedimentary rocks are
250 coarser and preferentially transported near the bottom of the river.
251

252 **5.2. Quantification of basaltic vs. crystalline material in the sediments**
253
254 Using the relationship between Nd and Hf isotopes as shown in Figure 5, we estimated the
255 proportion of basaltic erosion products at different water depths in the Yamuna and Chambal
256 sediments. As the Hf isotopic signature of the Deccan Traps basalts is poorly documented and no
257 Nd-Hf data have been reported in the literature for the area drained by the Chambal River (Figure

1); we performed our mixing calculations using two extreme values for the Deccan Traps endmember (see Figure 5a-b, and Supplementary Table 2 for more details). Both calculations give nevertheless similar results. Figure 5 shows that the Nd and Hf isotopic compositions of the Yamuna and Chambal sediments can be reproduced through mixing between radiogenic material eroded from the Deccan Traps (red squares in Figure 5) and sedimentary material sampled at different water depths in the Ganges River i.e. sediments that represent the erosion products of the Himalayan range and the northern Indian shield (yellow points in Figure 5). The surface suspended loads from both Yamuna and Chambal Rivers have the highest ε_{Nd} and ε_{Hf} values and are well explained by a contribution of 30-60% of Deccan Traps basalts associated to 40-70% of Ganges surface suspended loads, depending on which endmember is used for the Deccan Traps basalts (cf. Figure 5a-b). The slightly lower ε_{Nd} and ε_{Hf} values of deeper suspended loads require 20 to 50% of basaltic material. Finally, the bedloads and bank sediments from Yamuna and Chambal rivers resemble those of the Ganges River and include only 10-20% of Deccan Traps basalts. Our calculations thus quantitatively show that the proportion of basaltic erosion products decreases with depth in both rivers, demonstrating that bedloads and suspended loads sampled at the same location can record different provenances. To our knowledge, no publication reports similar data although Bouchez et al. (2011) mentioned the existence of a "provenance stratification" in the Amazon river based on Sr isotopic compositions of sediments.

Variations of Pb isotopic ratios in the Ganges, Yamuna and Chambal sediments are generally in agreement with Nd and Hf isotopic compositions even if things are slightly more ambiguous (Figure 3; Figure 6). The Deccan Traps basalts have relatively low $^{206\text{-}207\text{-}208}Pb/^{204}Pb$ while sediments from the Himalayan Range have generally higher but mainly more variable Pb isotopes. Here again, the Yamuna and Chambal sediments have generally less radiogenic signatures than the Ganges

River sediments, a feature consistent with a higher involvement of material deriving from the Deccan Traps basalts. However, the influence of the different sources on Pb isotopic ratios is blurred by the effect of hydrodynamic sorting that concentrates heavy minerals, such as zircon, monazite and allanite, with extremely radiogenic Pb isotopic ratios in the coarse sediments while fine-grained sediments, poorer in heavy minerals, have less radiogenic values (Garçon et al., 2013b, 2014). In addition, the large range of Pb isotopic compositions reported for the Deccan Traps basalts makes it impossible to calculate quantitative proportions of basaltic materials in the Yamuna and Chambal sediments (Figure 6).

5.3. Bias potentially introduced for provenance studies and crustal estimates

The extent of the provenance bias generated by erosion and sedimentary processes can be estimated by comparing the proportion of basalt exposed in the catchment areas of the Yamuna and Chambal Rivers to the proportion of basaltic material effectively present in the river sediments i.e. the proportion estimated above using Nd and Hf isotopic compositions. The Nd and Hf isotopic compositions of the Chambal bank sediment suggest that this sediment almost exclusively derives from the erosion of the Indian shield (Figure 5) and mixing calculations indicate that it includes less than 10% of basaltic material. In contrast, the Deccan Traps basalts represent about 30% of the drainage area at this sampling location (Figure 1). Similarly, the Deccan Traps basalts cover about 20% of the drained area at our Yamuna River site but our calculation indicates that the proportion of basaltic material in the bottom sediments is less than 20% (Figure 5). In both rivers, basaltic material is underrepresented in coarse-grained sediments. In contrast, surface suspended loads consist of 30-60% of material eroded from the Deccan Traps basalts for the Yamuna River and the Chambal River; hence basaltic material is overrepresented in fine suspended loads. Such

an isotopic bias has wider implications because it certainly also affects oceanic detrital sediments. Indeed, if as demonstrated here, eroded basalts are overrepresented in surface suspended loads delivered into the ocean at the mouths of large rivers, then, the contribution of basaltic material in oceanic terrigenous clays could be much higher than the proportion of basalts exposed to weathering on continents. Conversely, the basaltic precursor could be significantly underestimated in coarse terrigenous sediments such as turbidites deposited next to continental margins. The relative mass fluxes between fine-grained suspended load and coarse-grained bedload is not precisely known in the Chambal and Yamuna rivers but Jha et al. (1988) and Bawa et al. (2014) estimate that the suspended sediment flux at the outflow of the Yamuna River vary between 10 and 100 million tons per year depending on the sampling year, an amount that is not negligible when compared to the average total sediment flux of 400 million tons/year estimated by Lupker et al. (2011) at the outflow of the Ganges in Bangladesh. Furthermore, Lupker et al. (2012b) shows that the contribution of the Deccan Traps basalts in the Ganges sediments in Bangladesh is also highly variable from year to year, ca. 4% in 2007 and 2008 but up to 17% in 2005. This demonstrates that the flux of basalt-dominated suspended sediments can represent a non-negligible part of the total sediment flux that is discharged in the Bay of Bengal for certain years.

The overrepresentation of volcanic sources in oceanic sediments was highlighted 25 years ago by McLennan et al. (1989) and more recent work showed the preponderant role of chemical weathering of basalts on the composition of the seawater (Dessert et al., 2001; 2003). What our new results demonstrate is that rock erodibility, climate and river hydrodynamics affect the Nd, Hf and Pb isotopic compositions of detrital sediments to an extend that was not previously imagined. Our data suggests that the overestimation of basaltic material in fine-grained sediments could reach at least a factor of 2 (Figure 5). We acknowledge that, at the global scale, basalt exposures cover

328 only about 5% of the total continental surfaces (Amiotte Suchet et al., 2003), which may not be
329 enough to bias the overall isotopic composition of oceanic and continental sediments. We however
330 expect this effect to be significant for detrital sediments deposited next to subduction zones and
331 orogenic areas such as the Andes or the Cascades mountain ranges where significant amount of
332 basalts are exposed to weathering. The over/under-representation of basaltic erosion products
333 certainly also affect detrital materials discharged by several large river systems such as the Nile
334 River in Africa or the Parana River in South America where basalts cover respectively 20% and
335 12% of the total drainage area (Amiotte Suchet et al., 2003). All grain-size fractions, but not only
336 fine-grained sediments, should thus be considered in studies using Nd, Hf or Pb isotopic data to
337 trace the provenance of detrital sediments and their variations through time (e.g. Hemming and
338 McLennan, 2001; Li et al., 2003; Prytulak et al., 2006; Carpentier et al., 2008; Singh et al., 2008;
339 Carpentier et al., 2014). Our results also indicate that caution should be taken when using
340 sedimentary material as proxies to estimate the average isotopic compositions or ages of large
341 continental areas (e.g. Goldstein et al., 1984; Goldstein and Jacobsen, 1988; Asmerom and
342 Jacobsen, 1993; Plank and Langmuir, 1998; Millot et al, 2004; Garçon et al., 2011; Vervoort et al.,
343 2011; Chauvel et al., 2014) because the under/overrepresentation of volcanogenic sources could
344 significantly bias the derived average value depending on the type of sediment that is considered.
345

346 **6. Conclusions**

347 The data reported here reveal that bedload and suspended load sediments do not carry similar
348 provenance information when both basalts and crystalline rocks are exposed in the catchment area.
349 Large Nd, Hf and Pb isotopic differences exist between bedloads/bank sediments and suspended
350 loads sampled at different water depths in the Chambal and Yamuna Rivers draining basaltic,

crystalline and sedimentary rocks. In these rivers, basalt-derived materials are overrepresented in fine-grained sediments transported in suspension near the water surface while materials eroded from crystalline and sedimentary rocks are overrepresented in bedload/bank sediments. Mixing models suggest that the bias could be as large as a factor of 2. As river suspended load is a major contributor to the deep oceanic sedimentation, we suggest that basaltic materials may be also over-represented in fine-grained oceanic sediments and under-represented in coarse-grained turbidites. Finally, we emphasize the need to a careful evaluation of the Nd, Hf and Pb isotopic compositions of sediments when used as provenance proxies in both continental and oceanic environments.

Acknowledgments

We greatly thank Christian France-Lanord, Valier Galy and Maarten Lupker for the sediment sampling, Sarah Bureau for her help in the clean lab, Philippe Telouk for the assistance during MC-ICP-MS measurements at Lyon and Nick Arndt for constructive discussions that helped improving the content of the manuscript. We also thank Albert Galy and an anonymous reviewer for their constructive comments and Mark Harrison for his editor work. They all helped improving the clarity of the discussion. This study was supported by funding from CNRS and the University of Grenoble.

References

Albarède, F., Goldstein, S.L., Dautel, D., 1997. The neodymium isotopic composition of manganese nodules from the Southern and Indian oceans, the global oceanic neodymium budget, and their bearing on deep ocean circulation. Geochimica et Cosmochimica Acta 61, 1277–1291.

Albarède, F., Simonetti, A., Vervoort, J.D., Blichert-Toft, J., Abouchami, W., 1998. A Hf-Nd isotopic correlation in ferromanganese nodules. Geophys. Res. Lett. 25, 3895–3898.

374 Allègre, C.J., Rousseau, D., 1984. The Growth of the Continent Through Geological Time Studied
375 by Nd Isotope Analysis of Shales. Earth and Planetary Science Letters 67, 19–34.
376 Allègre, C.J., Dupré, B., Négrel, P., Gaillardet, J., 1996. Sr-Nd-Pb isotope systematics in Amazon
377 and Congo River systems: constraints about erosion processes. Chemical Geology 131, 93–
378 112.
379 Amiotte Suchet, P., Probst, J.-L., Ludwig, W., 2003. Worldwide distribution of continental rock
380 lithology: Implications for the atmospheric/soil CO_2 uptake by continental weathering and
381 alkalinity river transport to the oceans. Global Biogeochem. Cycles 17, 2, 1038.
382 Asmerom, Y., Jacobsen, S.B., 1993. The Pb isotopic evolution of the Earth: inferences from river
383 water suspended loads. Earth and Planetary Science Letters 115, 245–256.
384 Bawa, N., Jain, V., Shekhar, S., Kumar, N., Jyani, V., 2014. Controls on morphological variability
385 and role of stream power distribution pattern, Yamuna River, western India. Geomorphology,
386 in press, 1–13.
387 Bayon, G., Burton, K.W., Soulet, G., Vigier, N., Dennielou, B., Etoubleau, J., Ponzevera, E.,
388 German, C.R., Nesbitt, R.W., 2009. Hf and Nd isotopes in marine sediments: Constraints on
389 global silicate weathering. Earth and Planetary Science Letters 277, 318–326.
390 Belousova, E.A., Preiss, W.V., Schwarz, M.P., Griffin, W.L., 2006. Tectonic affinities of the
391 Houghton Inlier, South Australia: U – Pb and Hf-isotope data from zircons in modern stream
392 sediments. Australian Journal of Earth Sciences 53, 971–989.
393 Ben Othman, D., White, W.M., Patchett, J., 1989. The geochemistry of marine sediments, island
394 arc magma genesis, and crust-mantle recycling. Earth and Planetary Science Letters 94, 1–21.
395 Bouchez, J., Gaillardet, J., France-Lanord, C., Maurice, L., Dutra-Maia, P., 2011. Grain size control
396 of river suspended sediment geochemistry: Clues from Amazon River depth profiles.
397 Geochem. Geophys. Geosyst. 12, Q03008.
398 Bouvier, A., Vervoort, J.D., Patchett, P.J., 2008. The Lu–Hf and Sm–Nd isotopic composition of
399 CHUR: constraints from unequilibrated chondrites and implications for the bulk composition
400 of terrestrial planets. Earth and Planetary Science Letters 273, 48–57.
401 Carpentier, M., Chauvel, C., Mattielli, N., 2008. Pb–Nd isotopic constraints on sedimentary input
402 into the Lesser Antilles arc system. Earth and Planetary Science Letters 272, 199–211.
403 Carpentier, M., Chauvel, C., Maury, R.C., Mattielli, N., 2009. The "zircon effect" as recorded by
404 the chemical and Hf isotopic compositions of Lesser Antilles forearc sediments. Earth and

405 Planetary Science Letters 287, 86–99.
406 Carpentier, M., Weis, D., Chauvel, C., 2014. Fractionation of Sr and Hf isotopes by mineral sorting
407 in Cascadia Basin terrigenous sediments. Chemical Geology 382, 67–82.
408 Chauvel, C., Blichert-Toft, J., 2001. A hafnium isotope and trace element perspective on melting
409 of the depleted mantle. Earth and Planetary Science Letters 190, 137–151.
410 Chauvel, C., Bureau, S., Poggi, C., 2011. Comprehensive chemical and isotopic analyses of basalt
411 and sediment reference materials. Geostandards and Geoanalytical Research 35, 125–143.
412 Chauvel, C., Garçon, M., Bureau, S., Besnault, A., Jahn, B.-M., Ding, Z., 2014. Constraints from
413 loess on the Hf–Nd isotopic composition of the upper continental crust. Earth and Planetary
414 Science Letters 388, 48–58.
415 Chauvel, C., Marini, J.-C., Plank, T., Ludden, J.N., 2009. Hf-Nd input flux in the Izu-Mariana
416 subduction zone and recycling of subducted material in the mantle. Geochem. Geophys.
417 Geosyst. 10, Q01001.
418 Cina, S.E., Yin, A., Grove, M., Dubey, C.S., Shukla, D.P., Lovera, O.M., Kelty, T.K., Gehrels,
419 G.E., Foster, D.A., 2009. Gangdese arc detritus within the eastern Himalayan Neogene
420 foreland basin: Implications for the Neogene evolution of the Yalu–Brahmaputra River system.
421 Earth and Planetary Science Letters 285, 150–162.
422 Clift, P.D., Lee, J.I., Hildebrand, P., Shimizu, N., Layne, G.D., Blusztajn, J., Blum, J.D., Garzanti,
423 E., Khan, A.A., 2002. Nd and Pb isotope variability in the Indus River System: implications
424 for sediment provenance and crustal heterogeneity in the Western Himalaya. Earth and
425 Planetary Science Letters 200, 91–106.
426 Das, A., Krishnaswami, S., Sarin, M.M., Pande, K., 2005. Chemical weathering in the Krishna
427 Basin and Western Ghats of the Deccan Traps, India: Rates of basalt weathering and their
428 controls. Geochimica et Cosmochimica Acta 69, 2067–2084.
429 David, K., Frank, M., O'Nions, R., Belshaw, N., Arden, J., 2001. The Hf isotope composition of
430 global seawater and the evolution of Hf isotopes in the deep Pacific Ocean from Fe-Mn crusts.
431 Chemical Geology 178, 23–42.
432 Derry, L.A., and France-Lanord, C., 1996, Neogene Himalayan weathering history and river
433 $^{87}Sr/^{86}Sr$: impact on the marine Sr record: Earth and Planetary Science Letters, 142, 1, 59–74.
434 Dessert, C., Dupré, B., François, L.M., Schott, J., Gaillardet, J., Chakrapani, G., Bajpai, S., 2001.
435 Erosion of Deccan Traps determined by river geochemistry: impact on the global climate and

436 the 87Sr/86Sr ratio of seawater. Earth and Planetary Science Letters 188, 459–474.
437 Dessert, C., Dupré, B., Gaillardet, J., François, L.M., Allègre, C.J., 2003. Basalt weathering laws
438 and the impact of basalt weathering on the global carbon cycle. Chemical Geology 202, 257–
439 273.
440 Dhuime, B., Hawkesworth, C.J., Storey, C.D., Cawood, P.A., 2011. From sediments to their source
441 rocks: Hf and Nd isotopes in recent river sediments. Geology 39, 407–410.
442 Galer, S.J.G., Abouchami, W., 1998. Practical application of lead triple spiking for correction of
443 instrumental mass discrimination. Mineralogical Magazine 491–492.
444 Galy, A., France-Lanord, C., 2001. Higher erosion rates in the Himalaya: Geochemical constraints
445 on riverine fluxes. Geology 29, 23–26.
446 Galy, V., France-Lanord, C., Lartiges, B., 2008. Loading and fate of particulate organic carbon
447 from the Himalaya to the Ganga–Brahmaputra delta. Geochimica et Cosmochimica Acta 72,
448 1767–1787.
449 Galy, V., France-Lanord, C., Peucker-Ehrenbrink, B., Huyghe, P., 2010. Sr–Nd–Os evidence for a
450 stable erosion regime in the Himalaya during the past 12 Myr. Earth and Planetary Science
451 Letters 290, 474–480.
452 Garçon, M., Chauvel, C., Bureau, S., 2011. Beach placer, a proxy for the average Nd and Hf
453 isotopic composition of a continental area. Chemical Geology 287, 182–192.
454 Garçon, M., Chauvel, C., France-Lanord, C., Huyghe, P., Lavé, J., 2013a. Continental sedimentary
455 processes decouple Nd and Hf isotopes. Geochimica and Cosmochimica Acta, 121, 177-195.
456 Garçon, M., Chauvel, C., France-Lanord, C., Limonta, M., Garzanti, E., 2013b. Removing the
457 "heavy mineral effect" to obtain a new Pb isotopic value for the upper crust. Geochemistry
458 Geophysics Geosystems 14, 9. doi: 10.1002/ggge.20219
459 Garçon, M., Chauvel, C., France-Lanord, C., Limonta, M., Garzanti, E., 2014. Which minerals
460 control the Nd–Hf–Sr–Pb isotopic compositions of river sediments? Chemical Geology 364,
461 42–55.
462 Garzanti, E., Andò, S., France-Lanord, C., Censi, P., Pietro Vignola, Galy, V., Lupker, M., 2011.
463 Mineralogical and chemical variability of fluvial sediments 2. Suspended-load silt (Ganga–
464 Brahmaputra, Bangladesh). Earth and Planetary Science Letters 302, 107–120.
465 Garzanti, E., Andò, S., France-Lanord, C., Vezzoli, G., Censi, P., Galy, V., Najman, Y., 2010.
466 Mineralogical and chemical variability of fluvial sediments 1. Bedload sand (Ganga–

Brahmaputra, Bangladesh). Earth and Planetary Science Letters 299, 368–381.
Godfrey, L., Lee, D.-C., Sangrey, W., Halliday, A., Salters, V., Hein, J., White, W., 1997. The Hf isotopic composition of ferromanganese nodules and crusts and hydrothermal manganese deposits: Implications for seawater Hf. Earth and Planetary Science Letters 151, 91–105.
Goldstein, S., Jacobsen, S.B., 1988. Nd and Sr isotopic systematics of river water suspended material: implications for crustal evolution. Earth and Planetary Science Letters 87, 249–265.
Goldstein, S.L., O'nions, R.K., Hamilton, P.J., 1984. A Sm-Nd isotopic study of atmospheric dusts and particulates from major river systems. Earth and Planetary Science Letters 70, 221–236.
Hemming, S., McLennan, S., 2001. Pb isotope compositions of modern deep sea turbidites. Earth and Planetary Science Letters 184, 489–503.
Jha, P.K., Subramanian, V., Sitasawad, R., 1988. Chemical and sediment mass transfer in the Yamuna River--A tributary of the Ganges system. Journal of Hydrology 104, 237–246.
Jha, P.K., Vaithiyanathan, P., and Subramanian, V., 1993, Mineralogical characteristics of the sediments of a Himalayan river: Yamuna River - a tributary of the Ganges: Environmental Geology, 22, 13–20.
Kamber, B.S., Greig, A., Collerson, K.D., 2005. A new estimate for the composition of weathered young upper continental crust from alluvial sediments, Queensland, Australia. Geochimica et Cosmochimica Acta 69, 1041–1058.
Kramers, J.D., Tolstikhin, I.N., 1997. Two terrestrial lead isotope paradoxes, forward transport modelling, core formation and the history of the continental crust. Chemical Geology 139, 75–110.
Krishnan, M.S., 1982. Geology of India and Burna, 6 ed. CBS Publishers and Distributors, New Delhi.
Le Fort, P., 1975. Himalayas: the collided range. Present knowledge of the continental arc. American Journal of Science 275A, 1–44.
Li, X.-H., Wei, G., Shao, L., Liu, Y., Liang, X., Jian, Z., Sun, M., Wang, P., 2003. Geochemical and Nd isotopic variations in sediments of the South China Sea: a response to Cenozoic tectonism in SE Asia. Earth and Planetary Science Letters 211, 207–220.
Lupker, M., Blard, P.-H., lavé, J., France-Lanord, C., Leanni, L., Puchol, N., Charreau, J., Bourlès, D., 2012a. 10Be-derived Himalayan denudation rates and sediment budgets in the Ganga basin. Earth and Planetary Science Letters 333-334, 146–156.

498 Lupker, M., France-Lanord, C., Galy, V., lavé, J., Gaillardet, J., Gajurel, A.P., Guilmette, C.,
499 Rahman, M., Singh, S.K., and Sinha, R., 2012b. Predominant floodplain over mountain
500 weathering of Himalayan sediments (Ganga basin): Geochimica et Cosmochima Acta, 84,
501 410–432.

502 Lupker, M., France-Lanord, C., lavé, J., Bouchez, J., Galy, V., Métivier, F., Gaillardet, J., Lartiges,
503 B., Mugnier, J.-L., 2011. A Rouse-based method to integrate the chemical composition of river
504 sediments: Application to the Ganga basin. J. Geophys. Res. 116, F04012.

505 McLennan, S.M., McCulloch, M.T., Taylor, S.R., Maynard, J.B., 1989. Effects of sedimentary
506 sorting on neodymium isotopes in deep-sea turbidites. Nature 337, 547–549.

507 McLennan, S.M., Taylor, S.R., McCulloch, M.T., Maynard, J.B., 1990. Geochemical and Nd-Sr
508 isotopic composition of deep-sea turbidites: Crustal evolution and plate tectonic associations.
509 Geochimica et Cosmochimica Acta 54, 2015–2050.

510 Millot, R., Allègre, C.J., Gaillardet, J., Roy, S., 2004. Lead isotopic systematics of major river
511 sediments: a new estimate of the Pb isotopic composition of the Upper Continental Crust.
512 Chemical Geology 203, 75–90.

513 Padoan, M., Garzanti, E., Harlavan, Y., Villa, I.M., 2011. Tracing Nile sediment sources by Sr and
514 Nd isotope signatures (Uganda, Ethiopia, Sudan). Geochimica et Cosmochimica Acta 75,
515 3627–3644.

516 Parrish, R.R., Hodges, V., 1996. Isotopic constraints on the age and provenance of the Lesser and
517 Greater Himalayan sequences, Nepalese Himalaya. Geological Society of America Bulletin
518 108, 904–911.

519 Pearce, J., Kempton, P., Nowell, G., Noble, S., 1999. Hf-Nd element and isotope perspective on
520 the nature and provenance of mantle and subduction components in Western Pacific arc-basin
521 systems. Journal of Petrology 40, 1579–1611.

522 Plank, T., Langmuir, C.H., 1998. The chemical composition of subducting sediment and its
523 consequences for the crust and mantle. Chemical Geology 145, 325–394.

524 Prytulak, J., Vervoort, J.D., Plank, T., Yu, C., 2006. Astoria Fan sediments, DSDP site 174,
525 Cascadia Basin: Hf–Nd–Pb constraints on provenance and outburst flooding. Chemical
526 Geology 233, 276–292.

527 Rengarajan, R., Singh, S.K., Sarin, M.M., Krishnaswami, S., 2009. Strontium isotopes and major
528 ion chemistry in the Chambal River system, India: Implications to silicate erosion rates of the

529 Ganga. Chemical Geology 260, 87–101.
530 Richards, A., Argles, T., Harris, N., Parrish, R., Ahmad, T., Darbyshire, F., Draganits, E., 2005.
531 Himalayan architecture constrained by isotopic tracers from clastic sediments. Earth and
532 Planetary Science Letters 236, 773–796.
533 Roddaz, M., Viers, J., Brusset, S., Baby, P., Hérail, G., 2005. Sediment provenances and drainage
534 evolution of the Neogene Amazonian foreland basin. Earth and Planetary Science Letters 239,
535 57–78.
536 Rudnick, R.L., Gao, S., 2003. The Composition of the Crust, in: Rudnick, R.L. (Ed.), The Crust
537 Vol.3 Treatise on Geochemistry. pp. 1–64.
538 Singh, S.K., France-Lanord, C., 2002. Tracing the distribution of erosion in the Brahmaputra
539 watershed from isotopic compositions of stream sediments. Earth and Planetary Science
540 Letters 202, 645–662.
541 Singh, P., 2009. Major, trace and REE geochemistry of the Ganga River sediments: Influence of
542 provenance and sedimentary processes. Chemical Geology 266, 242–255.
543 Singh, S.K., Rai, S.K., Krishnaswami, S., 2008. Sr and Nd isotopes in river sediments from the
544 Ganga Basin: Sediment provenance and spatial variability in physical erosion. J. Geophys. Res.
545 113, F03006.
546 Steinmann, M., Stille, P., 2008. Controls on transport and fractionation of the rare earth elements
547 in stream water of a mixed basaltic–granitic catchment basin (Massif Central, France).
548 Chemical Geology 254, 1–18.
549 Tricca, A., Stille, P., Steinmann, M., Kiefel, B., Samuel, J., Eikenberg, J., 1999. Rare earth elements
550 and Sr and Nd isotopic compositions of dissolved and suspended loads from small river
551 systems in the Vosges mountains (France), the river Rhine and groundwater. Chemical
552 Geology 160, 139–158.
553 Van De Flierdt, T., Hemming, S.R., Goldstein, S.L., Abouchami, W., 2006. Radiogenic isotope
554 fingerprint of Wilkes Land–Adélie Coast Bottom Water in the circum-Antarctic Ocean.
555 Geophys. Res. Lett. 33, L12606.
556 Vance, D., Bickle, M., Ivy-Ochs, S., Kubik, P.W., 2003. Erosion and exhumation in the Himalaya
557 from cosmogenic isotope inventories of river sediments. Earth and Planetary Science Letters
558 206, 273–288.
559 Vervoort, J., Plank, T., and Prytulak, J., 2011, The Hf-Nd isotopic composition of marine

560 sediments. Geochimica et Cosmochimica Acta, 75, 5903-5926.
561 Vervoort, J.D., Patchett, P.D., Blichert-Toft, J., Albarède, F., 1999. Relationships between Lu–Hf
562 and Sm–Nd isotopic systems in the global sedimentary system. Earth and Planetary Science
563 Letters 168, 79–99.
564 Vlastélic, I., 2005. Miocene climate change recorded in the chemical and isotopic (Pb, Nd, Hf)
565 signature of Southern Ocean sediments. Geochem. Geophys. Geosyst. 6, Q03003.
566 White, W.M., Albarède, F., Télouk, P., 2000. High-precision analysis of Pb isotope ratios by multi-
567 collector ICP-MS. Chemical Geology 167, 257–270.
568 White, W.M., Patchett, J., BenOthman, D., 1986. Hf isotope ratios of marine sediments and Mn
569 nodules: evidence for a mantle source of Hf in seawater. Earth and Planetary Science Letters
570 79, 46–54.
571 Woodhead, J., Hergt, J., Davidson, J., Eggins, S., 2001. Hafnium isotope evidence for
572 "conservative" element mobility during subduction zone processes. Earth and Planetary
573 Science Letters 192, 331–346.
574 Wu, W., Xu, S., Yang, J., Yin, H., Lu, H., Zhang, K., 2010. Isotopic characteristics of river
575 sediments on the Tibetan Plateau. Chemical Geology 269, 406–413.
576
577

578 **Tables**

579

580 **Table 1:** Trace element concentrations and Nd-Hf-Pb of the Chambal, Yamuna and Ganges

581 sediments

582 ** Data already published by Garçon et al. (2013a ; 2013b)*

583 Uncertainties (± 2σ) reported in the Table for isotopic data correspond to in-run errors. ε_{Nd} and ε_{Hf}

584 were calculated using the CHUR composition of Bouvier et al. (2008).

585

586

587

Table 1

				Depth profile					
Sample Name	BR 935	BR 937	BR 938	BR 913	BR 912	BR 911	BR 914	*BR 717**	*BR 415**
Sampling date	14-Aug-09	14-Aug-09	14-Aug-09	9-Aug-09	9-Aug-09	9-Aug-09	9-Aug-09	*17-Aug-07*	*13-Jul-04*
Latitude (°N)	26.657	26.657	26.657	26.1306	26.1306	26.1306	26.1306	*24.0529*	*24.0529*
Longitude (°E)	77.903	77.903	77.903	79.7539	79.7539	79.7539	79.7539	*89.0247*	*89.0247*
River	Chambal	Chambal	Chambal	Yamuna	Yamuna	Yamuna	Yamuna	*Ganges*	*Ganges*
Type of sediment	Suspended load	Bank sediment	Bank sediment	Suspended load	Suspended load	Suspended load	Bedload	*Bedload*	*Suspended Load*
Sampling depth (m)	0			0.2	3.3	7.3	≈10	*11*	*0*
Cs	7.84	1.30	5.02	7.99	7.65	6.15	2.22	*3.87*	*15.4*
Rb	105	44.2	77.2	110	109	95.0	57.8	*50.3*	*202*
Ba	346	267	325	394	389	362	293	*244*	*627*
Th	12.0	15.8	9.50	11.6	12.8	13.5	20.1	*74.2*	*20.0*
U	1.95	2.29	1.69	2.73	2.23	2.62	3.69	*11.7*	*4.64*
Nb	13.6	8.24	10.5	14.1	14.2	14.9	14.6	*20.3*	*17.4*
Ta	1.00	0.655	0.783	1.05	1.08	1.15	1.35	*2.50*	*1.54*
La	28.7	34.0	24.2	27.5	30.5	35.8	51.1	*141*	*42.0*
Ce	62.6	68.7	54.1	61.0	69.2	78.5	107	*292*	*89.4*
Pr	6.95	8.06	6.03	6.66	7.52	8.64	11.8	*33.1*	*9.75*
Pb	23.1	14.0	17.5	24.9	28.0	21.3	16.6	*14.2*	*30.4*
Nd	27.2	30.2	23.2	25.3	28.6	32.2	43.1	*121*	*35.0*
Sr	204	132	180	193	172	167	160	*98.3*	*84.1*
Sm	5.57	5.69	4.65	5.20	5.71	6.50	8.24	*22.3*	*6.93*
Zr	133	383	159	144	177	276	621	*1550*	*178*
Hf	3.53	9.74	4.10	3.75	4.43	6.95	15.3	*40.5*	*4.73*
Ti	5415	3588	4334	5038	5118	5216	5019	*5299*	*4137*
Eu	1.23	0.902	1.08	1.16	1.18	1.26	1.29	*2.24*	*1.27*
Gd	4.86	4.63	4.39	4.76	5.18	5.53	6.61	*17.7*	*6.19*
Tb	0.751	0.69	0.664	0.754	0.78	0.839	1.01	*2.52*	*0.984*
Dy	4.74	4.24	4.12	4.52	4.75	5.03	5.96	*14.7*	*5.97*
Ho	0.935	0.814	0.809	0.898	0.911	0.999	1.14	*2.83*	*1.17*
Y	25.9	23.8	23.3	24.9	25.5	28.0	33.7	*85.6*	*32.7*
Er	2.62	2.34	2.33	2.59	2.59	2.82	3.40	*8.11*	*3.33*
Li	48.5	9.60	30.2	46.6	43.9	35.5	13.4	*15.7*	*51.8*
Yb	2.44	2.28	2.17	2.44	2.44	2.79	3.36	*8.17*	*3.18*
Lu	0.358	0.344	0.316	0.354	0.356	0.400	0.506	*1.25*	*0.461*
Sc	22.0	7.01	12.3	20.4	18.8	16.9	10.7	*14.3*	*15.0*
V	162	60.8	115	142	138	120	64.1	*53.5*	*93.4*
Cr	123	72.2	83.1	113	108	112	88.5	*44.1*	*76.6*
Co	25.7	6.00	18.1	22.5	20.6	17.1	6.82	*6.40*	*15.5*
Ni	83.5	19.5	52.3	74.1	67.4	53.1	19.1	*12.4*	*38.6*
Cu	106	20.5	54.8	98.2	73.0	47.0	16.9	*7.10*	*33.9*
Zn	125	23.5	57.2	157	187	73.9	34.2	*31.0*	*84.9*
$^{143}Nd/^{144}Nd \pm 2\sigma$	0.512122 ± 8	0.511779 ± 8	0.512038 ± 6	0.512101 ± 8	0.512051 ± 7	0.512008 ± 6	0.511835 ± 5	*0.511769 ± 7*	*0.511752 ± 6*
ε_{Nd}	-9.9	-16.6	-11.6	-10.3	-11.3	-12.1	-15.5	*-16.8*	*-17.1*
Duplicate									
$^{176}Hf/^{177}Hf \pm 2\sigma$	0.282656 ± 7	0.282101 ± 7	0.282426 ± 9	0.282605 ± 7	0.282506 ± 5	0.282340 ± 6	0.282140 ± 9	*0.281930 ± 6*	*0.282241 ± 9*
ε_{Hf}	-4.5	-24.2	-12.7	-6.4	-9.9	-15.7	-22.8	*-30.2*	*-19.2*
Re-run		0.282112 ± 9							
Duplicate							0.282139 ± 9		
$^{208}Pb/^{204}Pb \pm 2\sigma$	39.0273 ± 42	40.4987 ± 36	39.2603 ± 38	39.2302 ± 74	39.0014 ± 28	39.6362 ± 24	40.3682 ± 40	*42.4525 ± 26*	*40.3003 ± 18*
Re-run			39.2661 ± 26						
$^{207}Pb/^{204}Pb \pm 2\sigma$	15.7228 ± 12	15.8277 ± 14	15.7527 ± 12	15.7618 ± 24	15.7500 ± 8	15.8067 ± 8	15.8824 ± 12	*16.1109 ± 8*	*15.8991 ± 6*
Re-run			15.7536 ± 8						
$^{206}Pb/^{204}Pb \pm 2\sigma$	18.7124 ± 12	19.2689 ± 10	18.8164 ± 12	18.9519 ± 22	18.7890 ± 8	19.2948 ± 8	19.9554 ± 10	*22.1618 ± 10*	*20.0301 ± 6*
Re-run			18.8193 ± 8						

Table 1

	Depth profile						
Sample Name	*BR 414**	*BR 413**	*BR 412**	*BR 411**	*BR 418**	*BGP 6**	*BR 8253**
Sampling date	*13-Jul-04*	*13-Jul-04*	*13-Jul-04*	*13-Jul-04*	*13-Jul-04*	*2-Aug-96*	*10-Sep-08*
Latitude (°N)	*24.0529*	*24.0529*	*24.0529*	*24.0529*	*24.0529*	*24.3583*	*24.0529*
Longitude (°E)	*89.0247*	*89.0247*	*89.0247*	*89.0247*	*89.0247*	*88.6083*	*89.0247*
River	*Ganges*	*Ganges*	*Ganges*	*Ganges*	*Ganges*	*Ganges*	*Ganges*
Type of sediment	*Suspended Load*	*Suspended Load*	*Suspended Load*	*Suspended Load*	*Bedload*	*Bank sediment*	*Suspended Load*
Sampling depth (m)	*2*	*4*	*6.5*	*9*	*10*		*0*
Cs	*13.6*	*11.8*	*11.7*	*8.08*	*2.64*	*3.83*	*8.92*
Rb	*186*	*174*	*175*	*107*	*56.6*	*77.9*	*51.7*
Ba	*562*	*531*	*527*	*372*	*212*	*294*	*240*
Th	*19.0*	*19.3*	*18.0*	*15.1*	*29.7*	*30.2*	*16.1*
U	*4.08*	*4.15*	*3.96*	*2.92*	*5.14*	*5.41*	*1.85*
Nb	*17.9*	*16.5*	*15.7*	*13.6*	*18.4*	*12.9*	*15.8*
Ta	*1.57*	*1.45*	*1.39*	*1.37*	*2.08*	*1.78*	*1.31*
La	*41.3*	*42.2*	*40*	*32.8*	*71.0*	*67.1*	*30.8*
Ce	*88.1*	*89.2*	*84.7*	*76.3*	*146*	*144*	*75.4*
Pr	*9.77*	*9.87*	*9.29*	*7.84*	*16.7*	*15.5*	*8.12*
Pb	*26.2*	*25.3*	*25.3*	*17.4*	*15.0*	*17.8*	*10.5*
Nd	*35.7*	*35.8*	*34.0*	*29.0*	*60.4*	*56.5*	*31.2*
Sr	*91.0*	*99.3*	*101*	*88.6*	*103*	*115*	*56.5*
Sm	*6.98*	*7.01*	*6.77*	*5.60*	*12.0*	*10.9*	*6.27*
Zr	*204*	*227*	*199*	*249*	*479*	*683*	*196*
Hf	*5.22*	*5.79*	*5.17*	*6.14*	*12.1*	*17.1*	*5.13*
Ti	*4198*	*3976*	*3833*	*3314*	*4355*	*3155*	*4323*
Eu	*1.26*	*1.23*	*1.20*	*1.04*	*1.48*	*1.39*	*1.19*
Gd	*6.15*	*6.05*	*5.80*	*4.96*	*10.1*	*8.51*	*5.44*
Tb	*0.945*	*0.93*	*0.872*	*0.782*	*1.64*	*1.25*	*0.854*
Dy	*5.74*	*5.72*	*5.42*	*4.81*	*10.3*	*7.24*	*5.32*
Ho	*1.15*	*1.13*	*1.06*	*0.95*	*2.12*	*1.39*	*1.06*
Y	*32.8*	*32.5*	*30.9*	*27.1*	*62.0*	*41.1*	*31.1*
Er	*3.3*	*3.21*	*3.07*	*2.65*	*6.35*	*3.99*	*3.04*
Li	*48.2*	*43.5*	*41.9*	*32.2*	*15.8*	*14.7*	*45.3*
Yb	*3.11*	*3.06*	*2.88*	*2.51*	*6.23*	*3.87*	*2.95*
Lu	*0.45*	*0.448*	*0.417*	*0.366*	*0.905*	*0.587*	*0.433*
Sc	*14.4*	*13.5*	*12.8*	*9.04*	*13.2*	*7.74*	*11.8*
V	*90.7*	*81.1*	*79.1*	*61.8*	*46.9*	*32.7*	*100*
Cr	*81.9*	*67.0*	*63.4*	*53.4*	*40*	*36.9*	*73.6*
Co	*15.1*	*13.6*	*13.4*	*10.3*	*5.58*	*3.93*	*13.8*
Ni	*40.5*	*32.4*	*31.5*	*26.4*	*11.7*	*11.0*	*39.4*
Cu	*31.7*	*25.7*	*23.7*	*24.3*	*10.0*	*10.9*	*39.4*
Zn	*83.5*	*73.3*	*72.1*	*56.6*	*38.8*	*29.1*	*70.4*
$^{143}Nd/^{144}Nd \pm 2\sigma$	*0.511736 ± 8*	*0.511748 ± 6*	*0.511745 ± 7*	*0.511755 ± 6*	*0.511719 ± 5*	*0.511758 ± 9*	*0.511767 ± 8*
ε_{Nd}	*-17.4*	*-17.2*	*-17.3*	*-17.1*	*-17.8*	*-17.0*	*-16.8*
Duplicate				*0.511723 ± 7*			
$^{176}Hf/^{177}Hf \pm 2\sigma$	*0.282226 ± 6*	*0.282205 ± 6*	*0.282209 ± 6*	*0.282133 ± 7*	*0.281992 ± 11*	*0.282027 ± 11*	*0.282268 ± 7*
ε_{Hf}	*-19.8*	*-20.5*	*-20.4*	*-23.0*	*-28.1*	*-26.8*	*-18.3*
Re-run							
Duplicate							
$^{208}Pb/^{204}Pb \pm 2\sigma$	*40.3019 ± 24*	*40.2931 ± 34*	*40.2725 ± 16*	*40.1312 ± 28*	*40.8292 ± 24*	*40.6213 ± 44*	*39.9963 ± 28*
Re-run							
$^{207}Pb/^{204}Pb \pm 2\sigma$	*15.9013 ± 6*	*15.9040 ± 8*	*15.9040 ± 6*	*15.8984 ± 10*	*15.9684 ± 8*	*15.9733 ± 14*	*15.8730 ± 14*
Re-run							
$^{206}Pb/^{204}Pb \pm 2\sigma$	*20.0574 ± 8*	*20.0912 ± 8*	*20.0756 ± 8*	*20.0387 ± 10*	*20.6767 ± 10*	*20.7277 ± 14*	*19.7765 ± 10*
Re-run							

Figures

Figure 1: Map of the Ganges fluvial system showing where crystalline, sedimentary and basaltic rocks occur in the drainage basin.

Modified after Galy et al. (2010). Stars indicate the sampling locations of the sediments discussed in this study. See Table 1 for additional information on the location and nature of the different samples.

Figure 1

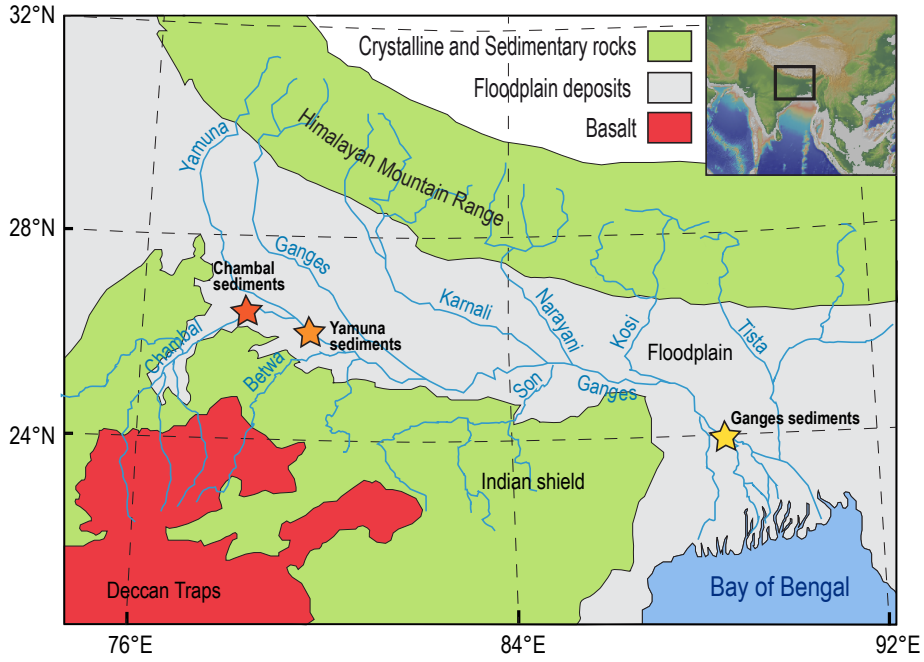

Figure 2: Trace element patterns of the Yamuna and Chambal sediments normalized to the composition of the upper continental crust (UCC) of Rudnick and Gao (2003). Bedloads and bank sediment are shown with grey lines while suspended loads are shown with black lines. The yellow field indicates the range of concentrations measured in the Ganges sediments in Bangladesh (data from Garçon et al. 2013a, see Table 1). The dashed gray line shows the trace element pattern of the outlier bank sediment BR 938 that resembles a suspended load.

Figure 2

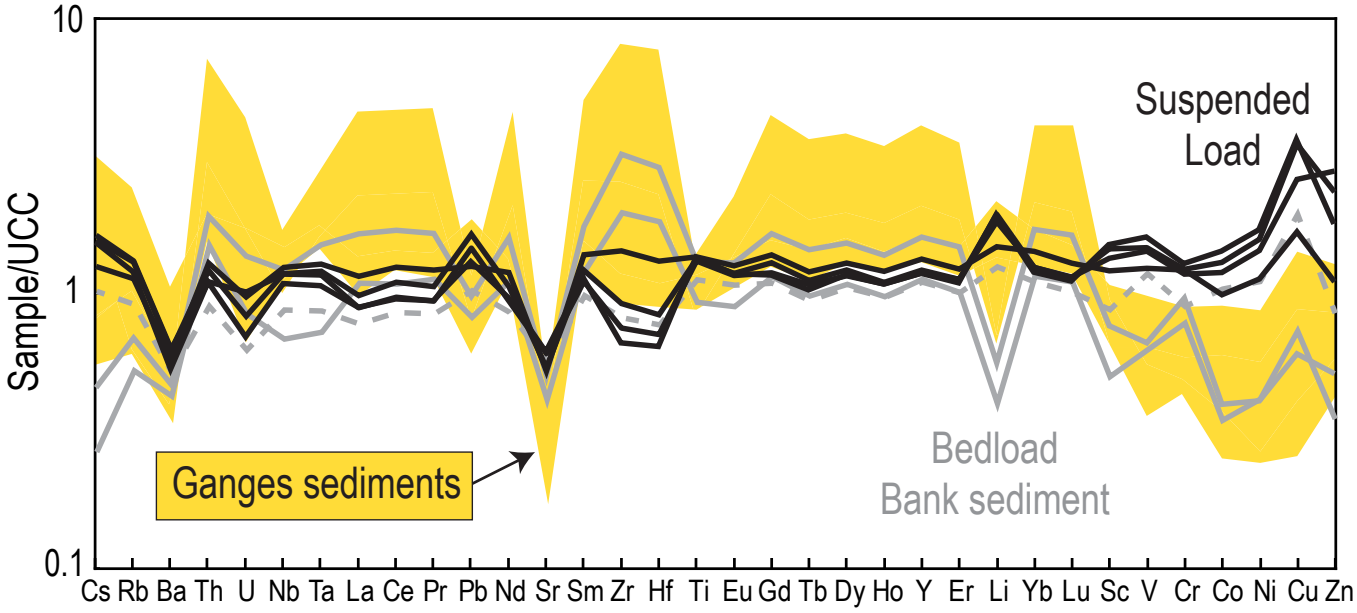

Figure 3: Nd, Hf and Pb isotopic variations of sediments sampled at different water depths in the Ganges, Yamuna and Chambal Rivers.

For the Ganges sediments, only samples recovered along the depth profile are shown in the diagrams (see Table 1; data from Garçon et al. 2013a, 2013b). The ranges of Nd, Hf and Pb isotopic ratios for all Himalayan sediments i.e. samples from the Ganges but also its major tributaries collected at different locations in the floodplain, from the Himalayan mountain front to the delta in Bangladesh are indicated by the green fields (data from Garçon et al. 2013a, 2013b). Red fields show the Nd, Hf and Pb isotopic compositions of the northern Deccan Traps basalts (data from the GEOROC database). River bank sediments are plotted at an arbitrarily depth of 10m. The dashed hexagon corresponds to the outlier bank sediment BR 938. ε_{Nd} and ε_{Hf} were calculated using the CHUR composition of Bouvier et al. (2008). Analytical errors are smaller than the symbol size except for Nd isotopes (horizontal bars at ± 0.5 ε units).

Figure 3

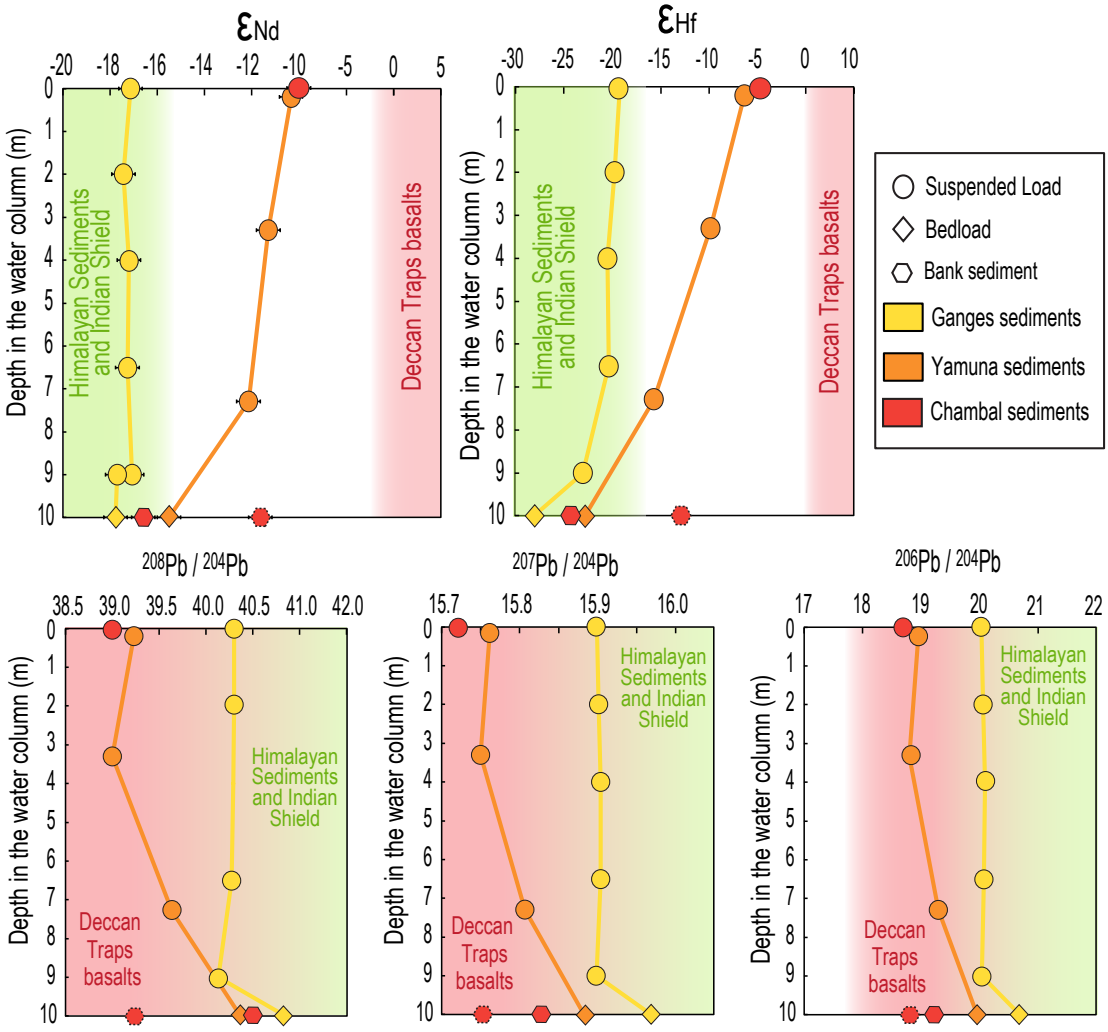
εNd
εHf
Depth in the water column (m)
Himalayan Sediments and Indian Shield
Deccan Traps basalts
Suspended Load
Bedload
Bank sediment
Ganges sediments
Yamuna sediments
Chambal sediments
208Pb / 204Pb
207Pb / 204Pb
206Pb / 204Pb
Himalayan Sediments and Indian Shield
Deccan Traps basalts

Figure 4: Variation of the La/Sm and Ni/Hf ratios as a function of depth for the Ganges, Chambal and Yamuna sediments.

As in Figure 3, only the Ganges sediments recovered along the depth profile are shown in the diagrams (see Table 1). Data for Himalayan sediments and Indian shield (green fields) are from Garçon et al. (2013a, 2013b). Blue vertical lines show the average La/Sm and Ni/Hf ratios for the upper continental crust (UCC) of Rudnick and Gao (2003). The red vertical line and the red field represent the average value and the range of values known for the northern Deccan Traps (data from the GEOROC database). River bank sediments were plot at an arbitrarily depth of 10m in each diagram. The dashed hexagon corresponds to the outlier bank sediment BR 938.

Figure 4

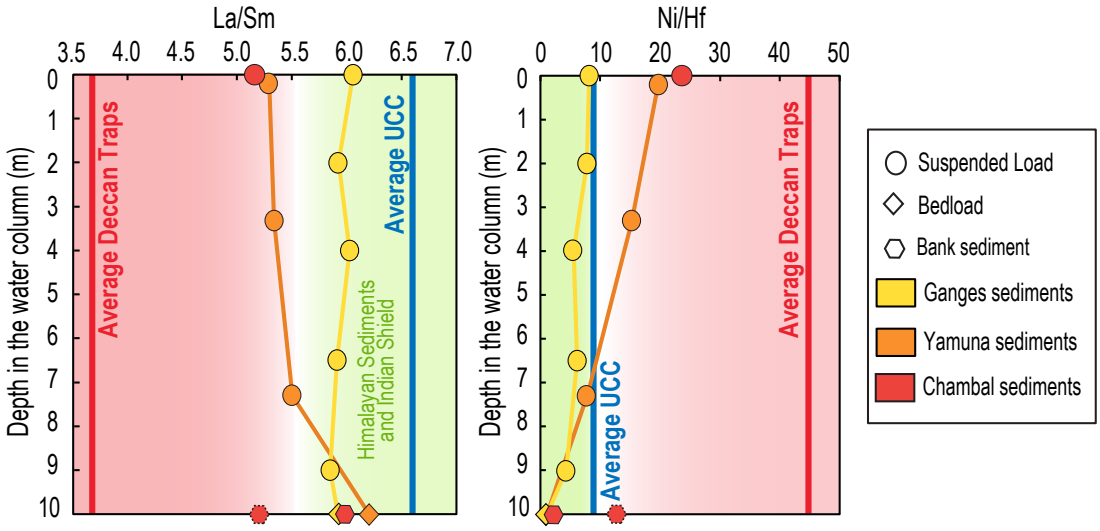

Figure 5: ε_{Nd} and ε_{Hf} diagrams showing the composition of the Ganges, Yamuna and Chambal sediments.

Black lines correspond to mixing curves between the Deccan Traps basalts and the sediments sampled at different water depths in the Ganges River in Bangladesh. Mixing calculations were performed using two extreme compositions for the Deccan Traps (see panel a) and b)). Ticks (every 10%) and associated numbers indicate the proportion of Deccan Traps basalts in the mixtures. The composition of the different endmembers used to calculate the mixing hyperbolas are summarized in Supplementary Table 2. The dashed hexagon corresponds to the outlier bank sediment BR 938 having Nd-Hf isotopic compositions similar to suspended loads. The present-day Terrestrial Array is that of Vervoort et al. (2011). Nd-Hf isotopic compositions of worldwide oceanic sediments are also shown. Data for Fe-Mn crusts and nodules are from Albarède et al. (1998), Godfrey et al. (1997), David et al. (2001), Van De Flierdt et al. (2006) and Albarède et al. (1997); oceanic clays and biogenic muds are from Bayon et al. (2009), McLennan et al. (1990), Ben Othman et al. (1989), Vervoort et al. (1999), White et al. (1986), Vlastélic (2005), Pearce et al. (1999), Woodhead et al. (2001), Prytulak et al. (2006), Carpentier et al. (2009), Chauvel et al. (2009), Vervoort et al. (2011) and Carpentier et al. (2008); finally, oceanic silts and sands are from Carpentier et al. (2008), Carpentier et al. (2009), McLennan et al. (1990), Vervoort et al. (1999), Bayon et al. (2009), Prytulak et al. (2006) and Vervoort et al. (2011). All ε_{Nd} and ε_{Hf} were recalculated using the CHUR composition of Bouvier et al. (2008). Analytical errors are smaller than the symbol size.

Figure 5

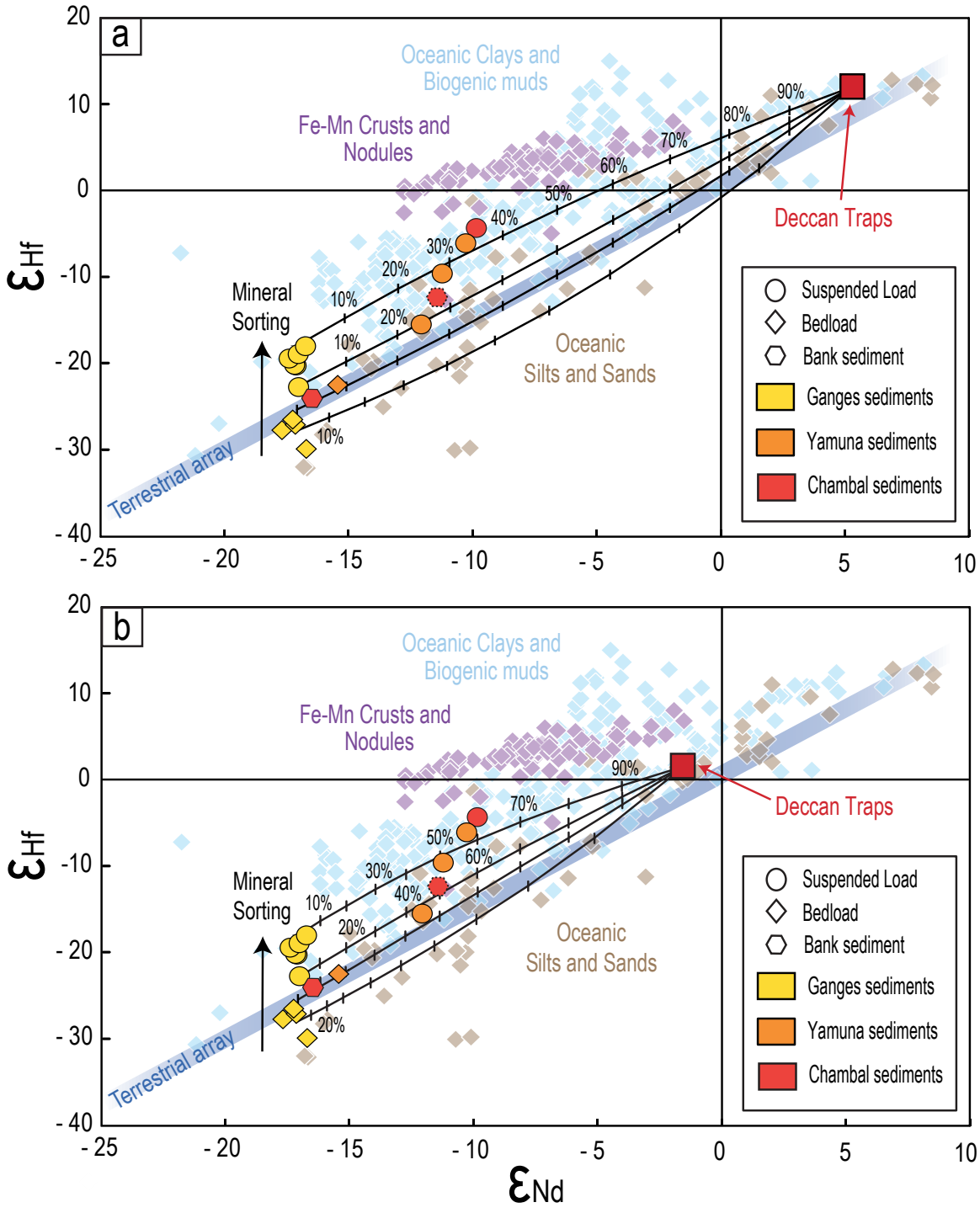
a
b
Oceanic Clays and Biogenic muds
Fe-Mn Crusts and Nodules
Deccan Traps
Mineral Sorting
Oceanic Silts and Sands
Terrestrial array
Suspended Load
Bedload
Bank sediment
Ganges sediments
Yamuna sediments
Chambal sediments
εHf
εNd

Figure 6: Pb isotopic compositions of the Ganges, Yamuna and Chambal sediments. Red triangles represent northern Deccan Traps basalts (data from the GEOROC database) while green triangles show the compositions of Himalayan sediments and Indian shield (data from Garçon et al., 2013b). The green star indicates the composition of the upper Himalayan crust as estimated by Garçon et al. (2013b). The dashed hexagon corresponds to the outlier bank sediment BR 938. Analytical errors are smaller than the symbol size.

Figure 6

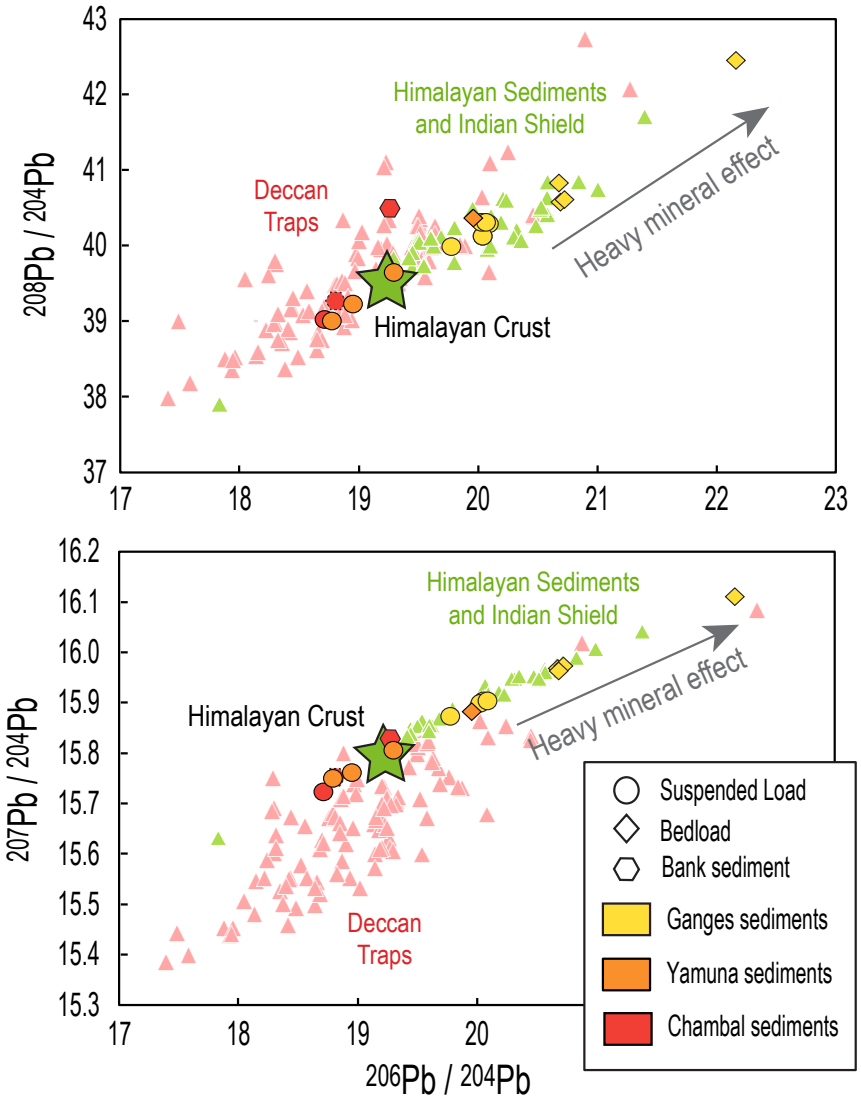

Supplementary Table 1: Trace-element concentrations measured in rock standards (ppm)

	BR reference *Chauvel et al. (2011)*	BR 24 reference *Chauvel et al. (2011)*	Average measured BEN n=4	2σ (%)	BEN *Chauvel et al. (2011)*	Diff (%)	Average measured JSd-2 n=6	2σ (%)	JSd-2 *Chauvel et al. (2011)*	Diff (%)
Li	15.1	7.15	13.2	7.5	13.0	1.5	22.6	2.7	22.1	2.3
Sc	22.8	25.9	22.6	3.6	22.5	0.4	17.4	2.1	17.9	-2.8
Ti	15300	17500	15382	3.5	15400	-0.1	3531	1.7	3570	-1.1
V	226	267	223	1.7	226	-1.2	124	1.2	126	-1.6
Cr	338	425	335	0.7	340	-1.4	100	1.0	106	-5.7
Co	56.6	52.6	59.0	0.8	60.0	-1.7	47.0	1.2	47.5	-1.1
Ni	259	238	256	0.3	258	-0.9	89.2	0.9	91.1	-2.1
Cu	68.8	37.0	64.5	4.0	69.3	-6.9	1061	4.6	1060	0.1
Zn	158	109	122	4.5	119	2.4	2138	0.9	1980	8.0
Rb	46.6	80.0	46.6	3.0	46.8	-0.5	25.6	1.3	25.8	-0.8
Sr	1340	607	1373	2.1	1380	-0.5	211	2.4	210	0.5
Y	28.9	28.5	28.8	0.7	29.0	-0.5	18.3	0.8	18.2	0.5
Zr	273	294	272	2.4	274	-0.6	107	0.5	103	3.9
Nb	115	38.1	119	4.9	116	2.6	4.44	1.8	4.19	6.0
Cs	0.82	0.648	0.75	5.1	0.752	-0.3	1.07	3.1	1.05	1.9
Ba	1090	390	1040	1.4	1050	-1.0	1225	3.3	1230	-0.4
La	82.6	33.6	82.5	0.8	83.0	-0.5	11.5	0.6	10.8	6.5
Ce	155	73.9	156	2.8	155	0.4	24.6	0.8	22.1	11.3
Pr	17.4	9.61	17.4	2.3	17.4	-0.1	3.08	1.1	2.94	4.8
Nd	66.4	39.9	66.1	2.3	67.0	-1.3	12.7	1.9	12.1	5.0
Sm	12.2	8.36	12.2	2.8	12.2	-0.2	2.97	2.1	2.86	3.8
Eu	3.66	2.53	3.66	2.3	3.67	-0.3	0.848	3.2	0.872	-2.8
Gd	9.88	7.28	9.87	1.0	9.87	0.0	3.14	2.0	2.85	10.2
Tb	1.25	1.03	1.25	2.9	1.26	-0.5	0.482	2.6	0.465	3.7
Dy	6.42	5.77	6.44	1.7	6.44	0.0	3.08	3.5	3.04	1.3
Ho	1.08	1.05	1.08	1.2	1.08	0.1	0.647	0.8	0.641	0.9
Er	2.58	2.70	2.59	0.8	2.59	-0.1	1.93	1.8	1.91	1.0
Yb	1.84	2.13	1.83	1.4	1.84	-0.4	1.94	1.9	1.91	1.6
Lu	0.246	0.297	0.241	2.4	0.245	-1.8	0.288	1.6	0.288	0.0
Hf	5.67	6.75	5.64	2.3	5.64	0.1	2.63	1.8	2.74	-4.0
Ta	5.55	2.34	5.98	2.4	5.57	7.3	0.366	2.7	0.345	6.1
Pb	4.77	3.69	4.52	4.9	4.17	8.3	166	0.6	154	7.8
Th	10.7	4.75	10.7	1.5	10.7	0.1	2.65	1.3	2.43	9.1
U	2.39	1.20	2.37	3.0	2.39	-0.7	1.09	1.2	1.09	0.0

Standard deviations (2σ) were calculated between the n measurements of the rock standards analysed as unknown samples and calibrated to the BR or BR 24 standards using the reference values of Chauvel et al. (2011). Differences between the published values and our measurements (Diff) are also reported in percentage. Note that differences between measured and published values are >5% for some elements in JSd-2. We attribute these differences to the heterogeneity of the standard (see Chauvel et al., 2011 and the GEOREM database for further details).

Supplementary Table 2: Endmembers for Nd-Hf isotopic mixings

	Hf (ppm)	ε_{Hf}	Nd (ppm)	ε_{Nd}
Ganges surface suspended load	4.5	-18.2	34	-17.2
Ganges intermediate suspended load	6	-23.1	34	-17.2
Ganges deep suspended load	7	-25.6	34	-17.2
Ganges bedload	14	-28.1	54	-17.2
Deccan Traps (Figure 5b) Low radiogenic endmember	4	1.6	20	-1.5
Deccan Traps (Figure 5a) Radiogenic endmember	4	11.8	20	5.3

The composition of the different mixing endmembers were constrained using the data of Garçon et al. (2013b) for the Ganges sediments and the data from Sen et al. (2009), Peng et al. (1998) and the GEOROC database for the Deccan Traps

Peng, Z.X., Mahoney, J.J., Hooper, P.R., Macdougall, J.D., and Krishnamurthy, P., 1998, Basalts of the northeastern Deccan Traps, India: isotopic and elemental geochemistry and relation to southwestern Deccan stratigraphy: Journal of Geophysical Research, v. 103, no. B12, p. 29,843–29,865.

Sen, G., Bizimis, M., Das, R., Paul, D.K., Ray, A., and Biswas, S., 2009, Deccan plume, lithosphere rifting, and volcanism in Kutch, India: Earth and Planetary Science Letters, v. 277, no. 1-2, p. 101–111, doi: 10.1016/j.epsl.2008.10.002